

Efficient Multiple Exciton Generation Observed in Colloidal PbSe Quantum Dots with Temporally and Spectrally Resolved Intraband Excitation

Minbiao Ji,^{†‡} Sungnam Park,[†] Stephen T. Connor,[§] Taleb Mokari,^{||} Yi Cui,[⊥] and Kelly J. Gaffney^{*†}

PULSE Institute SLAC National Accelerator Laboratory, Stanford University, Stanford, California 94305, Department of Physics, Department of Chemistry, and Department of Materials Science and Engineering, Stanford University, Stanford, California 94305, and Molecular Foundry, Lawrence Berkeley National Laboratory, Berkeley, California 94720

Received January 12, 2009

ABSTRACT

We have spectrally resolved the intraband transient absorption of photogenerated excitons to quantify the exciton population dynamics in colloidal PbSe quantum dots (QDs). These measurements demonstrate that the spectral distribution, as well as the amplitude, of the transient spectrum depends on the number of excitons excited in a QD. To accurately quantify the average number of excitons per QD, the transient spectrum must be spectrally integrated. With spectral integration, we observe efficient multiple exciton generation in colloidal PbSe QDs.

The generation of cost-effective and environmentally benign sources of energy represents a critical challenge for sustaining and advancing human well fair throughout the world while simultaneously reducing greenhouse gas emissions. Despite the tremendous potential of solar energy, the high cost of solar energy relative to conventional sources of electrical power limits solar energy to a minor component of the present global energy supply. This creates an enormous incentive to develop novel materials and approaches to light harvesting and power conversion.

The maximum single band gap solar cell conversion efficiency is calculated to be 31%, termed the Shockley-Queisser limit.¹ This calculation assumes that only one band edge electronic excited state can be generated per absorbed photon, with all photon energy in excess of the band gap energy being dissipated as heat. In bulk inorganic semiconductors this limitation has been shown to be an accurate assumption,² but the increased interaction between excitons in nanostructured inorganic semiconductors makes multiple exciton generation (MEG) potentially more efficient.³ Should efficient MEG and carrier extraction be achievable in a solar

cell, the theoretical photovoltaic device efficiency could be increased significantly to 43%.^{4,5}

The report of highly efficient MEG in PbSe QDs by Schaller and Klimov^{6,7} has stimulated significant interest in using MEG to improve photovoltaic efficiency. Ellingson et al.⁸ also observed efficient MEG in PbSe, and a variety of groups reported efficient MEG in a variety of semiconducting QDs.^{9–12} These initial claims, however, have been followed by a series of measurements that observe much weaker or nonexistent MEG.^{13–15}

Measurements in support of efficient MEG have been based primarily on time-resolved transient absorption (TA) measurements.^{6,8,16} A schematic of the experiment and data analysis method utilized to extract exciton multiplicity appears in Figure 1. In Figure 1A, the reduction in ground-state absorption, represented by the crossed-out upward green arrow, and the presence of stimulated emission, represented by the downward green arrow, result in an increased transmission of the probe pulse at the interband transition energy. When more than one exciton resides in a QD, the multiple exciton state decays quickly due to Auger recombination on the many tens to hundreds of picoseconds time scale,^{5,17–20} until only one exciton remains in the QD. In PbSe, this single exciton state decays radiatively on the hundreds of nanoseconds time scale,²¹ generating a nearly time-independent offset on the hundreds of picoseconds time

[†] PULSE Institute, SLAC National Accelerator Laboratory, Stanford University.

[‡] Department of Physics, Stanford University.

[§] Department of Chemistry, Stanford University.

^{||} Molecular Foundry, Lawrence Berkeley National Laboratory.

[⊥] Department of Materials Science and Engineering, Stanford University.

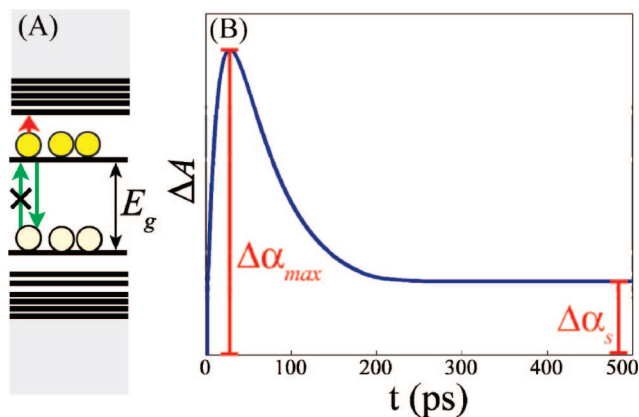


Figure 1. Schematic depiction of multiple exciton generation. (A) Electronic levels of the quantum dot, with loss of ground-state absorption at the band gap, E_g , shown as the crossed-out upward green arrow and stimulated emission as the downward green arrow. Excitons generation will lead to excited-state absorption (red arrow) in the mid-IR and a decreased absorption at the band gap energy. (B) As discussed in the text, the ratio of the maximum change in probe light transmission scaled by the long time change in transmission provides the exciton multiplicity.

scale, as shown in Figure 1B. This offset, $\Delta\alpha_s$, has been used as a proxy for the single exciton TA signal intensity and is used to scale the maximum change in absorption, $\Delta\alpha_{max}$, at early times to determine the average exciton multiplicity, $N_x = \Delta\alpha_{max}/\Delta\alpha_s$. This analysis assumes equal oscillator strength for the ground-state absorption and the stimulated emission and also assumes that the stimulated emission oscillator strength per exciton does not change when multiple excitons reside in a single QD. While these assumptions hold for weakly interacting excitons, the legitimacy of these assumptions has been brought into question for quantum-confined excitons.

The uncertain cross section for spontaneous and stimulated luminescence adds uncertainty to the interpretation of experimental data. Nair and Bawendi have performed time-resolved luminescence measurements and observed no evidence for efficient exciton multiplication in CdSe or PbSe QDs.^{15,22} Schaller et al.²³ have also performed time-resolved luminescence studies of exciton multiplication in CdSe QDs and conclude that time-resolved luminescence supports the conclusion that exciton multiplication occurs efficiently in CdSe. These CdSe luminescence studies are of particular relevance, since Klimov²³ and Bawendi¹⁵ observe similar experimental results but draw opposite conclusions regarding the efficiency of exciton multiplication. The dependence of the oscillator strength on exciton multiplicity for photon emission represents a key source of disagreement. For strongly confined excitons in a QD, the presence of two or more excitons will change the rate of spontaneous emission. The excited electrons will see multiple hole states into which the electrons can decay. Minimally, this results in a biexciton with twice the emission rate. Schaller et al.²⁴ account for this effect in their time-resolved luminescence study of CdSe. Nair et al.,¹⁵ however, conclude that the emission rate for a biexciton exceeded that of the monoexciton by a factor of 3–5 due to details in the electronic structure. In quantum

chemical calculations of the electronic transitions in CdSe,²⁵ Shumway, Franceschetti, and Zunger found that the transition dipole matrix elements for emission from the biexcitonic state exceeds that of the monoexcitonic state by roughly a factor of 9. The exciton multiplicity dependence of the emission cross section influences not only the spontaneous emission but also the stimulated emission, since the two processes involve the same transition dipole matrix elements.

Strong exciton–exciton interactions and electronic relaxation following photon absorption have the potential of generating very different stimulated emission cross sections for mono- and multiexciton states in transient absorption measurements.²⁶ Quantum mechanical calculations in PbSe QDs predict the first excited state to be weakly emissive, with a radiative decay dominated by thermal excitation to the strongly emissive second excited state.²⁷ As a consequence, the scaling used by Klimov and Nozik for transient absorption measurements performed at the band edge^{6,8} may be inappropriate since the cross section for stimulated emission from the biexciton may not be twice that of the single exciton. While the cross section for the ground-state bleach likely shows a comparatively weak exciton multiplicity dependence since the probe field will always connect optically active states within the probe pulse spectrum, the ground-state bleach and excited-state emission cannot be separated in a pump–probe measurement. This means that the exciton multiplicity dependent cross section for stimulated emission must be accounted for in the analysis of interband transition pump–probe measurements, not just in photoluminescence measurements of spontaneous emission.

The complexity of the electronic structure of QD^{25,27,28} and the uncertain impact this complexity has on the luminescence rate of multiple exciton states make it difficult to interpret the transient absorption measurements at the band gap energy and time-resolved luminescence measurements. We propose to avoid this difficulty by using the excited-state absorption to measure exciton populations and robustly determine the efficiency of MEG. This absorption will also be referred to as an intraband transition. Figure 1A schematically shows the excited-state absorption with an upward red arrow. This approach to characterizing multiple exciton generation has two significant advantages: the probed absorption (1) only exists in the presence of excited states and (2) will always connect optically active states assuming such transitions can be reached within the probe pulse spectrum. For PbSe QDs the excited-state absorption (intraband absorption) resides in the mid-IR.

Ellingson et al.⁸ used 5 μm probe light to measure the strength of the excited-state absorption and concluded from these measurements that exciton multiplication occurs with high efficiency. Ellingson et al. did not spectrally resolve the observed signal, though they did report that the transient behavior was not probe frequency dependent. This conclusion contrasts with the work of Wehrenberg et al.²⁰ where a significant shift in the intraband transient absorption spectrum occurred on the picosecond time scale. These time-dependent changes in the transient spectra can have significant impact on the extracted MEG efficiency. For the interband transition

in PbSe QDs, Trinh et al.²⁹ have demonstrated that spectral evolution can be significant and the accurate determination of the exciton multiplicity necessitates spectral integration. To clarify the importance of spectral dynamics on the intraband excited-state absorption, we have spectrally resolved the transient intraband absorption spectrum. These measurements clearly demonstrate that the intraband absorption spectrum displays a significant spectral evolution for triexcitonic and higher concentrations. As will be demonstrated, these spectral dynamics can have a significant impact on the interpretation of MEG when more than two excitons reside in a single QD.

Experimental Procedures. We followed the standard procedure of Talapin and Murray to prepare the PbSe QDs used in these experiments.³⁰ We precipitated the QDs from solution more than four times to remove the residual oleic acid to minimize the vibrational absorption of the oleic acid in the energy range of the probe pulse. We carefully dried the centrifuged QDs in a nitrogen gas stream and dissolved the QDs in carbon tetrachloride. The linear absorption spectrum shows a first exciton peak at 0.94 eV with a calculated diameter of 3.9 nm³¹ and a 10% size dispersion (see Supporting Information). We used a sample with optical density of 0.07 at 800 nm and 0.68 at 400 nm.

We generated pump and probe pulses with a regenerative amplified laser system (Spitfire, Spectra Physics) with a 1 kHz repetition rate and 35 fs full width at half-maximum (fwhm) pulse duration at 800 nm. We produced 400 nm pulses by frequency doubling the amplifier output with a 0.1 mm thick BBO crystal. Tunable mid-infrared pulses were generated by difference frequency generation of the near-infrared signal and idler from an optical parametric amplifier (OPA800CF, spectra physics). These mid-IR pulses have a duration of 60 fs fwhm with spectral width of about 300 cm⁻¹. Focusing these mid-IR pulses in a 2 mm thick Ge plate led to self-phase modulation and a significant broadening of the spectral width of the pulses. The probe spectrum (—) can be found in Figure 3A. This broadened spectrum provided an excellent probe with a spectral range extending from 1900 to 3100 cm⁻¹. We crossed the pump and probe beams in a 500 μm thick sample cell, with a probe diameter of 100 μm and a pump diameter of 400 μm at 800 nm and 3 mm at 400 nm. We used a static sample cell, without stirring³² or flowing of the sample in our measurements. The magnitude of the intraband absorption at negative time delays confirms that the steady state concentration of charged QD does not exceed 5%. We dispersed the probe beam with a grating spectrometer (iHR320, Horiba Jobin Yvon) onto a liquid N₂ cooled 32 × 2 MCT pixel array detector with a spectral resolution of 20 cm⁻¹ per pixel. The cross-correlation between the pump and probe pulse shows a duration of ~100 fs on each pixel.

Poissonian Behavior without MEG. A reliable study of MEG requires a correct measurement and control of the average number of photon absorbed per QD $N_0 = J_{\text{pump}}\sigma_\lambda$, where J_{pump} represents the pump laser fluence and σ_λ represents the absorption cross section at the pump wavelength. Here, we made use of the Poissonian absorption at

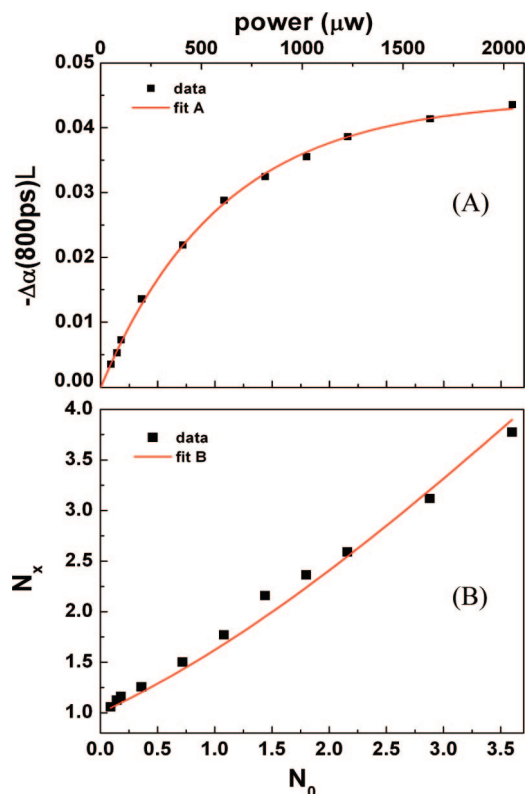


Figure 2. Poissonian behavior at pump photon energy below the MEG threshold. (A) TA at long delay time $-\Delta\alpha(800\text{ ps})L$ as a function of pump power and a fit using scheme A and eq 1. (B) Exciton multiplicity N_x as a function of pump power and a fit using scheme B and eq 2. Refer to the text for detailed discussion of the fitting schemes. We extract N_0 from the fits.

800 nm. A Poisson distribution of excitons results because two excitons cannot be generated from the absorption of a single 1.55 eV photon (~1.6 times the band gap energy). We did a careful pump power dependent measurement with spectral integration and extracted the value of the absorption cross section, σ_λ , using the linear relation between N_0 and the pump power. The Poisson distribution dictates both the early and long time signals, thus we utilized two fitting schemes to extract σ_λ . First, we focus on the long time TA signal. For small optical density, we have

$$-\Delta\alpha(800\text{ ps})L = N_{\text{QD}}L\sigma_{\text{probe}}(1 - e^{-N_0}) = C(1 - e^{-KP}) \quad (1)$$

where

$$K = \frac{\sigma_\lambda}{(\pi D^2/4)(hc/\lambda)f}$$

and P represents the pump power (μW), f the laser repetition rate (1 kHz), D the pump beam diameter at the sample (400 μm), and λ the pump wavelength (800 nm).

A fit of the data to eq 1 yields $K = (1.8 \pm 0.2) \times 10^{-3} \mu\text{W}^{-1}$, as shown in Figure 2A. Alternatively, the maximum TA can be used to extract σ_λ . The standard method for determining the maximum number of excitons per excited QD, N_x , takes the maximum change in absorption, $\Delta\alpha(2\text{ ps})$, and scales this transient signal by the change in absorption, $\Delta\alpha(800\text{ ps})$, at a time delay where Auger recombination has

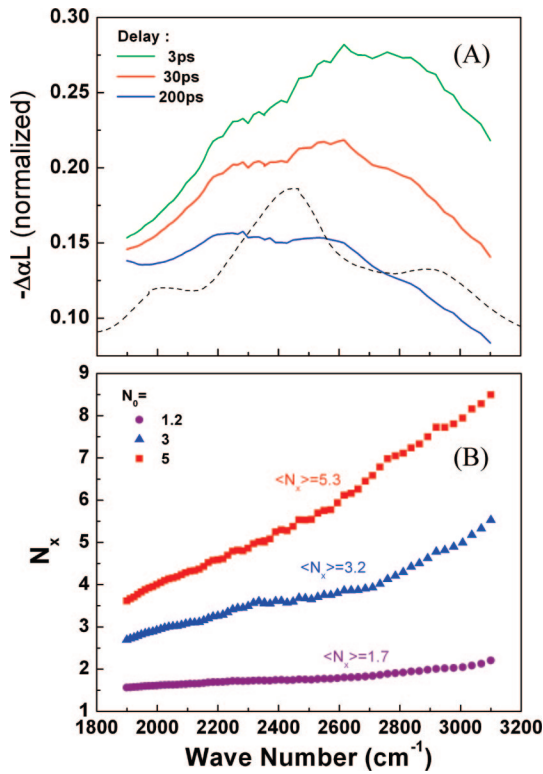


Figure 3. Spectrally resolved intraband TA data. (A) Experimental TA spectra at different probe delay times, the spectra at longer delay times do not differ from the one at 200 ps. The dashed line represents the broad probe spectrum. (B) Calculated exciton multiplicity N_x vs probe frequency for various pump powers (expressed in terms of N_0). We annotate these pump power dependent curves with the spectrally integrated multiplicity, $\langle N_x \rangle$.

eliminated all multiple exciton states, but before appreciable radiative recombination, $N_x = \Delta\alpha(2 \text{ ps})/\Delta\alpha(800 \text{ ps})$. This exciton multiplicity is given by

$$N_x = \frac{\Delta\alpha(2 \text{ ps})}{\Delta\alpha(800 \text{ ps})} = \frac{N_0}{1 - e^{-N_0}} = \frac{KP}{1 - e^{-KP}} \quad (2)$$

A fit of the data to eq 2 generates $K = (1.9 \pm 0.1) \times 10^{-3} \mu\text{W}^{-1}$ as shown in Figure 2B. Both methods provide very similar values for K from which we estimate $\sigma_{800\text{nm}} = 5.6 \pm 0.7 \text{ \AA}^2$. Furthermore, by using the relative absorption at 800 and 400 nm, we can determine the cross section at 400 nm to be $\sigma_{400\text{nm}} = 54 \pm 7 \text{ \AA}^2$, similar to the theoretical value³¹ of $\sigma_{400\text{nm}} = 60 \text{ \AA}^2$.

Time and Spectrally Resolved Excitonic Intraband Absorption. With a higher 800 nm pump fluence and $N_0 = 3-5$, the intraband absorption spectrum clearly evolves with time. This can be clearly seen in Figures 3–5. As mentioned above, the standard method for determining the average number of excitons per excited QD, $N_x = \Delta\alpha(2 \text{ ps})/\Delta\alpha(800 \text{ ps})$. As shown in Figure 3, the spectral dynamics makes N_x probe frequency dependent. The TA signal decay faster at higher frequencies, and the spectral difference becomes more significant with larger N_0 . Integrating the TA spectra alleviates this problem and demonstrates the insensitivity of the intraband absorption cross section to the exciton multiplicity. Assuming that only one exciton can be generated from the absorption of a single 800 nm photon, the average number

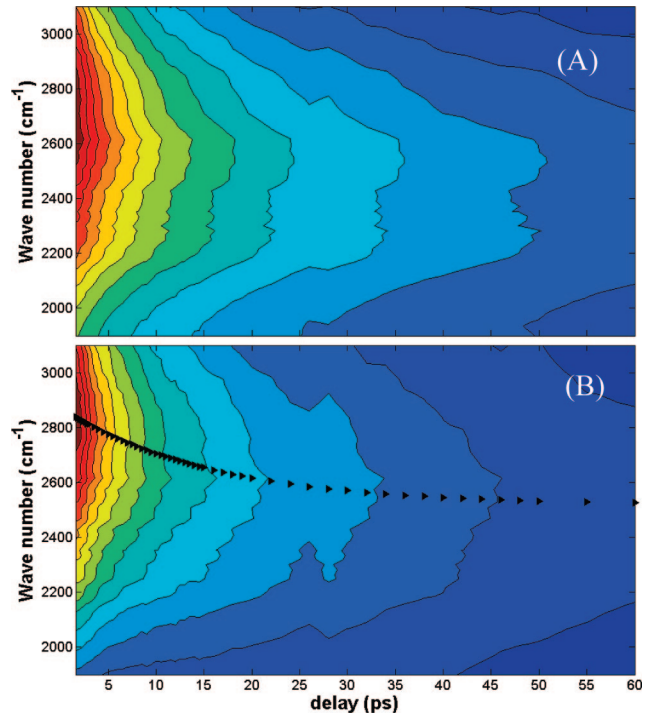


Figure 4. Two-dimensional pump-probe data at $N_0 = 5$. (A) Experimental TA signal as a function of probe delay time and frequency. (B) The resultant data after the feature with a time delay independent spectrum has been subtracted.

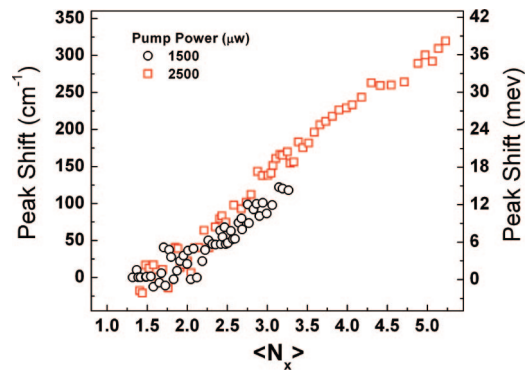


Figure 5. Exciton multiplicity dependent peak shift for the signal displayed in Figure 4B. We extract N_x from the spectrally integrated TA traces. The figure shows two pump powers for comparison.

of excitons per QD will be determined by the sample depth averaged N_0 . As can be seen in Figure 2B, the N_x and N_0 excitonic concentrations exhibit the expected correlation predicted by eq 2 over a wide range of excitonic multiplicity. This clearly demonstrates that the intraband absorption remains proportional to the number of excitons for multiplicities up to four and supports using the spectrally resolved intraband transition to characterize the exciton multiplicity in PbSe QDs.

Inspection of the TA spectrum shown in Figure 4 supports the assignment of the transient signal to two components. One component has a spectrum that does not evolve with time and can be accurately modeled by the intraband absorption spectrum measured at long time delays when only monoexcitonic states persist. The second component has been modeled with a Gaussian line shape that possesses a time-

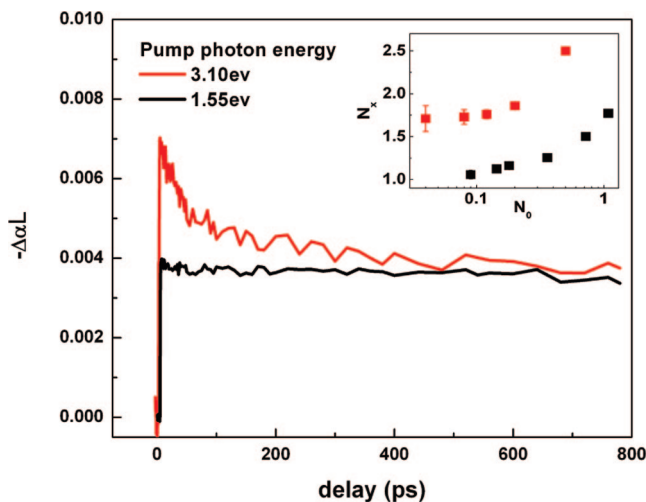


Figure 6. Data indicating the occurrence of MEG. TA traces measured with 1.55 and 3.1 eV pump photon energies at low photon fluences. We chose pump powers so that the long time TA tails roughly overlap. Inset shows the power scaling of the exciton multiplicities at the two pump photon energies.

dependent peak shift. Figure 4B shows the time dependence of this second Gaussian component. In order to link the magnitude of the peak shift to the number of excitons per excited dot, we correlate the two for each delay time. Spectral integration of the 2D transient gives a time-dependent multiplicity $N_x(t)$, and the fitting of the second component gives time-dependent peak position $\omega_0(t)$; thus we can correlate ω_0 and N_x . Interestingly, a significant shift in the peak position only occurs when the average number of excitons per QD exceeds 2. This can be seen in Figure 5, which shows the time-dependent spectral component peak maximum as a function of N_x . We believe the time-dependent spectrum results from Coulomb and exchange interactions between excitons, though further studies must be performed to confirm and characterize the origin of this apparent time-dependent electronic structure. These data clearly indicate that for MEG in excess of two excitons per QD, spectral integration must be performed to accurately determine the exciton multiplicity. In the following discussion of MEG, we have spectrally integrated the intraband transient absorption to determine the exciton multiplicity.

Investigation of Multiple Exciton Generation. We have investigated MEG in PbSe with laser excitation at 400 nm, which corresponds to 3.26 times the PbSe band gap energy of 0.94 eV. As we have emphasized, accurate determination of the MEG efficiency requires a probe signal that is proportional to the number of excitons per QD and spectral integration of the transient signal to effectively account for population-dependent spectral shifts in the transient signal. The accurate determination of the MEG efficiency also requires assurance that electron and hole trap states do not influence the TA signal and robust demonstration that $N_0 \ll 1$. We do not believe trap states play an important role in our measurements for two reasons. One, we see no evidence of traps when exciting with low fluence at 800 nm. This can be seen in Figure 6, where the 800 nm signal has no time dependence for short delay times. Most importantly, we can

use the magnitude of the mid-IR absorption at negative time delays to determine the concentration of charged QD. This measurement insures we have a charged QD concentration of less than 5%.

We have used multiple methods to ensure that $N_0 \ll 1$. Figure 6 shows the TA signal for low fluence excitation at 800 and 400 nm. The absence of any early time signal in the 800 nm signal ensures that $N_0 \ll 1$ at 800 nm and the overlap of the 800 and 400 nm generated signals at long delay times provides evidence that the same number of photons has been absorbed at 400 nm.²⁹ However, this might be insufficient, since the average number of absorbed photons depends on the optical thickness

$$\langle N_0 \rangle_L = N_0 \frac{1 - e^{-\alpha L}}{\alpha L}$$

Instead of using $\langle N_0 \rangle_L$, we took the more stringent quantity, N_0 . This ensures that the number of photons absorbed per QD at the front surface of the sample will also be much less than 1. Given the different absorptions at 400 and 800 nm used in the experiment, $\langle N_0 \rangle_L$ must be a factor of 2 lower at 400 nm to achieve the same N_0 .

As shown in the inset of Figure 6, we observe a laser fluence independent exciton multiplicity when exciting at 400 nm greater than 1, confirming the presence of MEG. For a photon energy equal to $3.26 E_g$, we observe an average of 1.6 ± 0.2 excitons per absorbed photon. This MEG efficiency matches the efficiency observed by Schaller et al. when exciting at 400 nm and using a PbSe QD with a similar E_g ,^{6,19,22} and exceeds the efficiency measured by Ellingson et al. at the same photon energy in a PbSe QD with a similar E_g .⁸ As emphasized by Nair and Bawendi,²² this efficiency does not significantly exceed the bulk efficiency measured by Smith and Dutton at 3.1 eV photon energy.³³ Whether quantum confinement has a significant impact on the observed efficiency cannot be assessed yet.²²

The creation and harvesting of multiple carriers from a single photon absorption represent an appealing and potentially important route to increasing the conversion efficiency of photovoltaic devices. While we remain far from identifying how to efficiently extract the generated carriers from the photoexcited quantum dots, before tackling such a difficult scientific and engineering challenge, we need to verify MEG efficiency warrants the effort. We believe the spectrally resolved intraband transition provides an excellent means of characterizing the efficiency of multiple exciton generation in PbSe and also provides an excellent opportunity to investigate the physical and chemical properties of PbSe QDs that determine the efficiency. At a minimum our results support further investigation and provide reason for optimism that multiple exciton generation may provide a valid means of enhancing solar cell efficiency beyond the Shockley–Queisser limit.

Acknowledgment. The work has been supported by the Global Climate and Energy Project (GCEP) at Stanford University, the King Abdullah University of Science and Technology (KAUST): Global Research Partnership (GRP) through the Center for Advanced Molecular Photovoltaics

(CAMP), and the Department of Energy. S.T.C. acknowledges the support from a National Science Foundation Graduate Fellowship. Work at the Molecular Foundry was supported by the Director, Office of Science, Office of Basic Energy Science, Division of Materials Science and Engineering, U.S. Department of Energy, under contract DE-AC02-05CH11231.

Supporting Information Available: The linear absorption spectrum and TEM images of the sample used in the experiment. This material is available free of charge via the Internet at <http://pubs.acs.org>.

References

- (1) Shockley, W.; Queisser, H. J. *J. Appl. Phys.* **1961**, *32* (3), 510–518.
- (2) Wolf, M.; Brendel, R.; Werner, J. H.; Queisser, H. J. *J. Appl. Phys.* **1998**, *83* (8), 4213–4221.
- (3) Nozik, A. J. *Annu. Rev. Phys. Chem.* **2001**, *52*, 193–231.
- (4) Werner, J. H.; Kolodinski, S.; Queisser, H. J. *Phys. Rev. Lett.* **1994**, *72* (24), 3851–3854.
- (5) Klimov, V. I. *Appl. Phys. Lett.* **2006**, *89* (12), 3.
- (6) Schaller, R. D.; Klimov, V. I. *Phys. Rev. Lett.* **2004**, *92* (18), 186601.
- (7) Schaller, R. D.; Agranovich, V. M.; Klimov, V. I. *Nat. Phys.* **2005**, *1* (3), 189–194.
- (8) Ellingson, R. J.; Beard, M. C.; Johnson, J. C.; Yu, P.; Micic, O. I.; Nozik, A. J.; Shabaev, A.; Efros, A. L. *Nano Lett.* **2005**, *5* (5), 865–871.
- (9) Beard, M. C.; Knutsen, K. P.; Yu, P.; Luther, J. M.; Song, Q.; Metzger, W. K.; Ellingson, R. J.; Nozik, A. J. *Nano Lett.* **2007**, *7* (8), 2506–2512.
- (10) Schaller, R. D.; Pietryga, J. M.; Klimov, V. I. *Nano Lett.* **2007**, *7* (11), 3469–3476.
- (11) Pijpers, J. J. H.; Hendry, E.; Milder, M. T. W.; Fanciulli, R.; Savolainen, J.; Herek, J. L.; Vanmaekelbergh, D.; Ruhman, S.; Mocatta, D.; Oron, D.; Aharoni, A.; Banin, U.; Bonn, M. *J. Phys. Chem. C* **2007**, *111* (11), 4146–4152.
- (12) Luther, J. M.; Beard, M. C.; Song, Q.; Law, M.; Ellingson, R. J.; Nozik, A. J. *Nano Lett.* **2007**, *7* (6), 1779–1784.
- (13) Ben-Lulu, M.; Mocatta, D.; Bonn, M.; Banin, U.; Ruhman, S. *Nano Lett.* **2008**, *8* (4), 1207–1211.
- (14) Pijpers, J. J. H.; Hendry, E.; Milder, M. T. W.; Fanciulli, R.; Savolainen, J.; Herek, J. L.; Vanmaekelbergh, D.; Ruhman, S.; Mocatta, D.; Oron, D.; Aharoni, A.; Banin, U.; Bonn, M. *J. Phys. Chem. C* **2008**, *112* (12), 4783–4784.
- (15) Nair, G.; Bawendi, M. G. *Phys. Rev. B* **2007**, *76* (8), 081304.
- (16) Jeffrey, M. H.; Hui, D.; Todd, D. K.; Kyung-Sang, C.; Chris, B. M.; Frank, W. W. *Phys. Rev. B* **2005**, *72* (19), 195312.
- (17) Klimov, V. I.; McGuire, J. A.; Schaller, R. D.; Rupasov, V. I. *Phys. Rev. B* **2008**, *77* (19), 195324.
- (18) Klimov, V. I.; Mikhailovsky, A. A.; Xu, S.; Malko, A.; Hollingsworth, J. A.; Leatherdale, C. A.; Eisler, H. J.; Bawendi, M. G. *Science* **2000**, *290* (5490), 314–317.
- (19) Schaller, R. D.; Petruska, M. A.; Klimov, V. I. *Appl. Phys. Lett.* **2005**, *87* (25), 3.
- (20) Wehrenberg, B. L.; Wang, C.; Guyot-Sionnest, P. *J. Phys. Chem. B* **2002**, *106* (41), 10634–10640.
- (21) Du, H.; Chen, C. L.; Krishnan, R.; Krauss, T. D.; Harbold, J. M.; Wise, F. W.; Thomas, M. G.; Silcox, J. *Nano Lett.* **2002**, *2* (11), 1321–1324.
- (22) Nair, G.; Geyer, S. M.; Chang, L. Y.; Bawendi, M. G. *Phys. Rev. B* **2008**, *78* (12), 10.
- (23) Schaller, R. D.; Sykora, M.; Pietryga, J. M.; Klimov, V. I. *Nano Lett.* **2006**, *6* (3), 424–429.
- (24) Schaller, R. D.; Sykora, M.; Jeong, S.; Klimov, V. I. *J. Phys. Chem. B* **2006**, *110* (50), 25332–25338.
- (25) Shumway, J.; Franceschetti, A.; Zunger, A. *Phys. Rev. B* **2001**, *63* (15), 13.
- (26) Fidler, H.; Terpstra, J.; Wiersma, D. A. *J. Chem. Phys.* **1991**, *94* (10), 6895–6907.
- (27) An, J. M.; Franceschetti, A.; Zunger, A. *Nano Lett.* **2007**, *7* (7), 2129–2135.
- (28) An, J. M.; Franceschetti, A.; Dudiy, S. V.; Zunger, A. *Nano Lett.* **2006**, *6* (12), 2728–2735.
- (29) Trinh, M. T.; Houtepen, A. J.; Schins, J. M.; Hanrath, T.; Piris, J.; Knulst, W.; Goossens, A. P. L. M.; Siebbeles, L. D. A. *Nano Lett.* **2008**, *8* (6), 1713–1718.
- (30) Talapin, D. V.; Murray, C. B. *Science* **2005**, *310* (5745), 86–89.
- (31) Moreels, I.; Lambert, K.; De Muynck, D.; Vanhaecke, F.; Poelman, D.; Martins, J. C.; Allan, G.; Hens, Z. *Chem. Mater.* **2007**, *19* (25), 6101–6106.
- (32) McGuire, J. A.; Joo, J.; Pietryga, J. M.; Schaller, R. D.; Klimov, V. I. *Acc. Chem. Res.* **2008**, *41* (12), 1810–1819.
- (33) Smith, A.; Dutton, D. *J. Opt. Soc. Am.* **1958**, *48* (12), 1007–1009.

NL900103F